S. Becker, T. Ranzani, S. Russo, R. J. Wood. "Pop-Up Tissue Retraction Mechanism for Endoscopic Surgery",
The 2017 IEEE/RSJ International Conference on Intelligent Robots and Systems (IROS 2017)

Pop-Up Tissue Retraction Mechanism for Endoscopic Surgery*

S. Becker[1], T. Ranzani[2], S. Russo[2], R. J. Wood[2]

Abstract— **Numerous therapeutic transendoscopic procedures exist to treat lesions in the GI tract. However, these procedures are limited by their difficulty and the amount of training required to successfully perform them. The surgeon is tasked with simultaneously steering the distal tip of the endoscope, applying tension to tissue to retract it, and manipulating electro-cautery tools with limited dexterity. We propose a device designed to assist with anchoring and tissue retraction during endoscopic surgical procedures. The designed solution decouples the tissue-grasping function from the movement of the endoscope tip, leaving the surgeon free to use the endoscope tip solely for positioning of electro-cautery or biopsy tools deployed through the endoscope working channel. The anchoring and retraction device uses pop-up book MEMS techniques, allowing for a "flat" structure to expand into a 3-D structure . The proposed device has three main integrated components: a rigid expandable geometric structure, inflatable pneumatic actuators, and a vacuum gripper. These inflatable actuators include internal rigid discs, allowing for resistance to buckling while maintaining the benefits of the established lightweight, low profile actuator design scheme. Proof-of-concept *ex vivo* testing demonstrates that the integrated device can be used to retract tissue to a height of 13.5 mm, providing access for endoscopy tools to contact a sample of porcine stomach tissue.**

I. INTRODUCTION

Current trends in surgical procedures have focused on minimally invasive surgery (MIS) with the end goal of shortening recovery time and improving patient outcomes. Since their development in the 1960s, flexible and steerable endoscopes have become the standard approach for diagnostic and therapeutic procedures in the gastrointestinal (GI) tract [1]. Although endoscopic diagnostic procedures performed are well-established and routine, many challenges exist when using endoscopes for therapeutic procedures, such as excising or ablating cancerous sites or other lesions. These challenges include distal tip instability, a lack of control for fine distal positioning, and the low amount of force that can be exerted by the endoscope tip without causing deflection of the endoscope itself [2]. Techniques such as endoscopic submucosal dissection (ESD) have been developed to help address these shortcomings [3], but they require extensive training to successfully perform. Endoscopic mucosal resection (EMR) is another procedure aimed at removing small lesions ($<$ 25 mm) in the GI tract, but is challenged by the lack of endoscope distal tip dexterity [3]. Additional research has included the development of endoscopic add-ons to supplement the existing capabilities of conventional endoscopes [4]–[8], but these are similarly hampered by the inherent flexibility of the endoscope. Although this flexibility is crucial for navigating the curving GI tract to reach the surgical site, the flexibility of the distal tip of the endoscope limits the capabilities of endoscopic therapeutic procedures [2], [9].

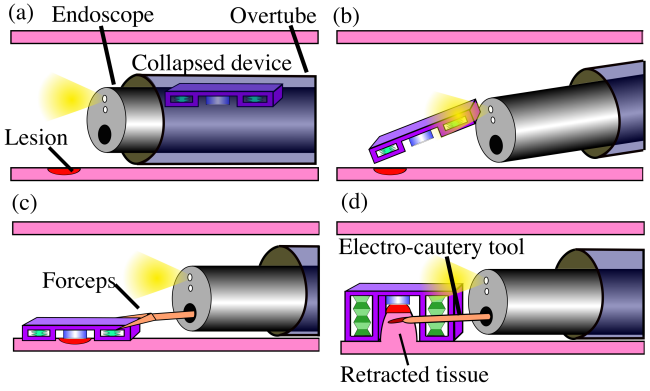

Fig. 1. Illustration of usage case of the proposed device and the workflow for deployment and tissue retraction: (a) collapsed device affixed to endoscope within hollow overtube, (b) deployment by retracting the overtube to expose the device, (c) positioning of the device with forceps over the targeted lesion, and (d) mechanism retracting tissue, allowing conventional tools to be used to excise the lesion with electro-cautery.

In this paper, we address the limitations of current resection or ablation-based surgical procedures targeting early colorectal cancer (ECC) lesions in the lower GI tract performed with conventional flexible endoscopes. In order to fit within the current workflow of therapeutic endoscopic procedures, the proposed tissue retraction device can be introduced into the body along the outside of the distal end of an endoscope and encased in a retractable overtube (Fig. 1). By automating the act of placing tissue under tension and decoupling this action from the motion of the endoscope tip, the integrated device presented here has the potential to expand surgeons' capabilities and increase the number of surgeons capable of performing these types of procedures.

*This work was supported by Harvard, the Wyss Institute for Biologically Inspired Engineering, and DARPA (award number FA8650-15-C-7548).

[1] S. Becker is with Harvard College at Harvard University, Cambridge, MA, 02138 USA samuelbecker@college.harvard.edu

[2] T. Ranzani, S. Russo, and R. J. Wood are with the John A. Paulson School of Engineering and Applied Sciences at Harvard University, Cambridge MA 02138, USA, and also with the Wyss Institute for Biologically-Inspired Engineering, Boston, MA 02115, USA tranzani, srusso, rjwood@seas.harvard.edu

In Section II. we introduce a fabrication scheme for embedding rigid disks in TPE bellows actuators based upon prior work [10], with planar manufacturing techniques. We also introduce the fabrication of an integrated device consisting of an expandable structure, inflatable bellows actuators, and a vacuum gripper to enable tissue retraction. The expandable structure is based upon the pop-up book MEMS fabrication methodology [11]. Pop-up book MEMS has been used successfully for the development of medical devices in the literature [12]. The concept of integrating soft, inflatable devices with expandable rigid structures to constrain the inflation of the actuator has also been previously proposed [8] [13]. The integrated device and its components are tested with protocols presented in Section III. and the results of these experiments are presented in Section IV.

II. DESIGN & FABRICATION

A. Concept Design

The proposed device can be affixed to the outside surface of the distal end of an endoscope and constrained within an overtube to shield the device from contacting tissue until at the surgical site in the GI tract, as shown in Fig. 1 (a). The overtube is then retracted to expose the device (Fig. 1 (b)). Forceps deployed through the endoscope working channel are used by the surgeon to position the device atop a lesion, with visual guidance and confirmation from the illuminated distal camera (Fig. 1 (c)). Although shown here placing the device on a horizontal section of tissue, the distal endoscope position and orientation can be adjusted by the surgeon to place the device in the GI tract regardless of orientation to horizontal because it is grasped by forceps during positioning. Once properly positioned, negative pressure is applied to the vacuum gripper at the center of the device, adhering the device to the lesion site while negative pressure is sustained. The dual bellows actuators are then inflated, expanding the pop-up structure and retracting the grasped tissue. The surgeon can now use conventional endoscopy tools such as electro-cautery probes inserted through the endoscope working channel to cut through the mucosa and muscularis layers beneath the lesion site, as shown in Fig. 1 (d). The dissected tissue is still held by the device's vacuum gripper and can be grasped with forceps for removal from the body for pathology analysis. The device is rapidly collapsed by venting pressure from the bellows actuators. To excise larger lesions, the device is repeatedly expanded, collapsed, and repositioned with forceps delivered through the endoscope working channel to adjust vacuum gripper location between rounds of electro-cautery. To remove the device from the body upon completion of a procedure, negative pressure is applied to the bellows actuators to keep them in a deflated state, the overtube is advanced, and forceps are used to maneuver the device back into the overtube while the endoscope is retracted. The thickness of the device before inflation should add less than 10 mm to the endoscope diameter to maintain overtube compatibility, and the device requires an expanded height of 13 mm or greater to retract tissue to a height of 10 mm, which offers sufficient access to the retracted tissue by endoscope end-effectors.

B. Bellows Actuator Design and Improvements

Heat- and pressure-bonded Thermoplastic Elastomer, TPE (Fiber Glast, USA) bellows actuators with Polytetrafluoroethylene (PTFE) mask layers have been developed that demonstrate a linear relationship between blocked force and input pressure at low displacement heights, but exert limited retractive forces due to the tendency of bellows chambers to buckle inwards when vacuum is applied, rather than move axially [10]. Here we propose the introduction of rigid PTFE disks within the enclosed chambers of the soft bellows actuators at the same scale. The planar fabrication method of combining subunits to form complete bellows chambers enables the inclusion of additional bellows chambers and thus customizable inflation height. This paper will focus on bellows actuators with a diameter of 9 mm and four connected bellows chambers. These dimensions were selected for suitability for integration into the tissue retraction device and limits on overtube size. The first sub-unit of the soft bellows actuator is fabricated with two adjacent layers of 38 μm thick TPE following the process shown in Fig. 2. This double layer of TPE enhances robustness of the material when undergoing deformation during heating, as this deformation is required to accommodate internal disks of sufficient thickness to resist buckling under applied negative pressure. Different layers of TPE are cut with a CO_2 laser cutter and alternated with laser-cut 254 μm and 76.2 μm PTFE layers to act as masks and forms. Layers of TPE and PTFE are aligned using precision dowel pins and stacked manually. The layers of TPE in the first two steps of the process are bonded at 180°C for one hour under 0.07 MPa pressure, as shown in Fig. 2. The 76.2 μm PTFE layers serve in the first step to mask the TPE and allow only desired areas to bond (Fig. 2 (a)). This first step produces the layer that interfaces between two bellows chambers. The 254 μm PTFE also serves as a mask to the TPE as well as a form to create sufficient vertical space while the TPE is heated to encase rigid PTFE disks within the bellows chambers.

During the second step of the process (Fig. 2 (b)), multiple subunits resulting from the first step may be added, serving to customize expanded height of the finished actuator. Additional 254 μm PTFE mold layers are added to transmit the vertically applied force of 0.07 MPa to the areas of TPE being bonded. In this

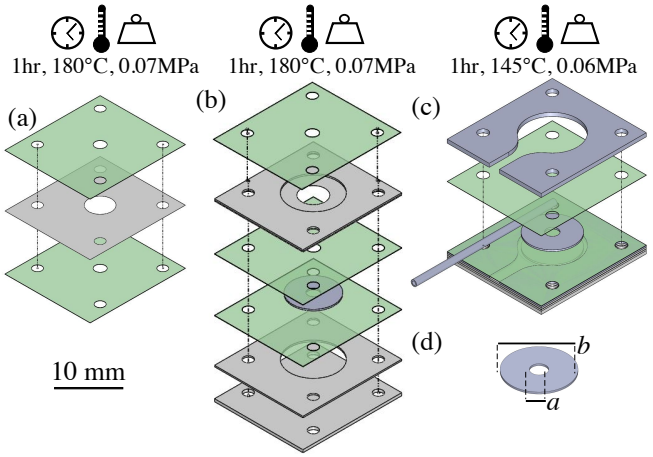

Fig. 2. Fabrication workflow for the proposed bellows actuators with internal rigid disks: (a) Interface layer between adjacent bellows chambers (b) Additional mold layers with the result of the previous step, creating pocket for enclosed disk (c) Final bonding of top TPE layer and input tubing (d) Enclosed disk dimensions. TPE layers are represented in green and TPFE layers are in gray

step, the bonds around the outer diameter of all bellows chambers except that with the inlet tubing are formed. Following heat- and pressure-bonding, the top layers of this laminate are manually removed, and additional 254 μm PTFE layers are added as forms to create bonds that will enclose the last bellows chamber with its inlet tubing. A tube with internal diameter of 0.64 mm (Micro Renathane Cather Tubing, Braintree Scientific, USA) is inserted and a drop of Loctite Vinyl, Fabric & Plastic Flexible Adhesive is added before the top sheet of TPE and an upper PTFE mold layer are added. The resulting laminate is heated at 145°C for one hour under 0.06 MPa pressure, as shown in Fig. 2 (c). The external PTFE layers are manually cut away before the laminate has cooled, and the inlet tubing is trimmed, producing bellows actuators like those shown in Fig. 3 (a).

The output force of an actuator produced from this process can be modeled by the simple $F = P \times A$ relationship, where F is the force produced, P is the input pressure, and A is the area of the circular bellows chamber when flat, as determined by the 254 μm PTFE layers that transmit the applied force during heating in Fig. 2 (b) and (c). This relationship holds true when expanding from flat, with decreased force output as the overall height increases and the TPE begins to strain. However, as this outputted force magnitude diminishes, $\Delta F = \Delta P$ x A is a better description. The rate at which force output increases with an increase in pressure will be relatively constant and dependent upon the area of a bellows chamber, and is detailed in Section IV.

Previous iterations of soft bellows actuators fabricated with a 76.2 μm PTFE film disk encased in each bellows chamber (solely to mask the TPE layers from bonding in the chamber) were susceptible to bending and buckling when under applied negative pressure, limiting the pulling force output to 0.50N [10]. Bellows actuators under retraction also undergo a time-dependent decay in applied force as they approach a steady-state constant output when the TPE and 76.2 μm PTFE have buckled to their minimum internal volume. As such, it was hypothesized that the incorporation of a thicker, more rigid PTFE disk would minimize these effects and improve the retraction performance of the actuator. Modeling the system as a disk under uniform radial compression, which the TPE would apply to the disk under applied negative pressure, as discussed in Eqn. 1, supports this hypothesis.

Based upon *Roark's Formulas for Stress and Strain* [14], we model the enclosed disk as a circular plate with a concentric hole under uniform radial compression on its outer edge, with a being outside diameter of the disk, b being the inner diameter of the disk as shown in Fig. 2 (d), t being thickness of the disk, E being Young's modulus, v being Poisson's ratio, and σ' being critical unit compressive stress. Because the ratio of diameter to thickness $\frac{a}{t}$ is greater than 10, this model holds and we can say that:

$$\sigma' = K(\frac{E}{1-v^2})^2(\frac{t}{a})^2 \tag{1}$$

where K is a tabulated value dependent upon $\frac{b}{a}$ and equal to a linearly interpolated value of 0.285, thus $\sigma' \propto t^2$, meaning that the resistance to buckling is proportional to the square of the thickness of the disk.

Therefore, increasing the thickness of the internal PTFE disks from 76.2 μm to a thicker sheet suggests that the bending stiffness of a chamber of the bellows actuator would increase by $(t_{thick}/t_{thin})^2$. Thus, when increasing disk thickness from 76.2 μm to 254 μm, this results in increased resistance to buckling by a factor of 3.3^2, or 10.89.

This assumes both versions are subjected to the same radial compression, as both are tested under equal vacuum line pressure applied to actuators that are identical other than thickness of their enclosed disks. A thicker internal disk, then, will allow individual bellows actuator chambers to resist subsequent buckling under vacuum and therefore allows higher retractive forces to be achieved.

C. Vacuum Grippers

In order to integrate the vacuum gripper into the laminar fabrication methodology of the pop-up structure, the mold is designed to yield a flat sheet of cast elastomer at the top of the vacuum gripper which could be mechanically constrained between two structural sheets with a pass-through for the tubing through which negative pressure is applied. Molds are 3D-printed on an SLA Formlabs 2 (Formlabs, Somerville, MA, USA). A silicone elastomer, DragonSkin 20 (Smooth-On, Macungie, PA, USA), is cast

into the molds and placed into a vacuum chamber until all trapped air escapes after about ten minutes, before being cured at 60°C for 60 minutes. Tubing with internal diameter of 0.64 mm (Micro Renathane Cather Tubing, Braintree Scientific, USA) is inserted and the connection is sealed with additional uncured DragonSkin 20 applied on the interior side of the seal with the vacuum gripper, as shown in Fig. 3 (b).

D. Pop-up Structure

Pop-up book MEMS is a design and fabrication methodology in which thin layers of material are machined individually and selectively laminated together with adhesive and flexible layers, allowing a flat structure to expand into a 3-dimensional device based on flexure joints [11]. The pop-up structure presented here is designed to accommodate the incorporation of a vacuum gripper and strain-relieving expandable housing for two bellows actuators, without substantial deformation during use. Materials for the fabrication of the pop-up structure include 381 μm thick fiberglass-epoxy laminate sheets as structural material (Garolite G-10/FR4), 25 μm thick polyimide film as flexure layers, and pressure-sensitive 3M® sheet adhesive (9877). Each layer is individually machined using a diode-pumped solid state (DPSS) laser, and aligned using precision dowel pins. The resulting laminate is laser machined to release the final device structure, shown in Fig. 3 (c) from the bulk substrate before integration of the vacuum gripper.

E. Integrated System

The bellows actuators with internal rigid PTFE disks and vacuum gripper are incorporated into the pop-up structure to complete the device, as shown in Fig. 3 (d) and (e). The vacuum gripper is mechanically constrained between two layers of fiberglass-epoxy laminate sheets. The bellows actuators are affixed on the top and bottom TPE layers with the same adhesive sheet. Input tubing lines for the bellows actuators are linked together by a tee-fitting to operate from a single input pressure line.

III. EXPERIMENTS

All subsystems of the integrated device were tested and characterized individually before incorporation into the integrated device. The soft bellows actuators with rigid internal disks were characterized both in expansion and retraction, a working range of output forces by vacuum suckers was experimentally determined, and the pop-up structure was measured to ensure suitable geometry. *Ex vivo* tests using porcine stomach were performed to simulate the use of the integrated device in the GI tract. The device was also affixed to an endoscope and a proof-of-concept deployment method was demonstrated. The burst pressure of the actuators was measured by pressuring actuators to failure and was found to be 299 kPa.

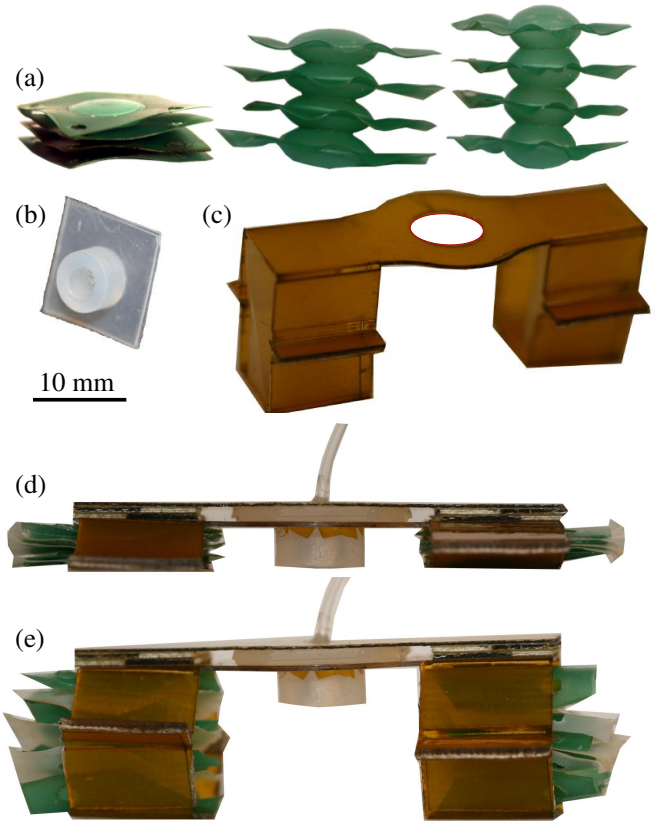

Fig. 3. Several subsystems are integrated together in the final device: (a) A four-stage TPE bellows actuators with rigid internal disks (shown in various stages of expansion), to expand the device (b) A silicone elastomer vacuum gripper, to grip the tissue to be retracted (c) The pop-up book MEMS structure comprised of structural, flexural, and adhesive layers. These are laminated together to create the final device (d) Integrated device in undeployed state (e) Integrated device fully expanded by inflated bellows actuators.

A. Bellows Actuator Force Characterization

A four-stage bellows actuator was tested on a materials testing machine (Instron®) by placing it between two flat rigid plates displaced from one another at various discrete heights. Dual syringe pumps provide controllable input pressure measured by a pressure gauge (BSP B010-EV002-A00A0B-S4, Balluff, USA), and force readings from the load cells (Instron® $\pm$ 10N Static Load Cell, Cat. No: 2530-428) were taken at regular pressure intervals. These values were compared to the theoretical model. The top and bottom layers of TPE were adhered to 254 μm fiberglass-epoxy laminate sheets with sheets of 3M® 9877 adhesive. This was done to cause a constant area of the TPE pressing against the fiberglass-epoxy laminate, and therefore also the Instron® plate and load cell, regardless of expansion.

Bellows actuators were also tested under applied negative pressure to determine the efficacy of the rigid PTFE disks contained within each chamber in resisting

buckling and exerting forces under applied negative pressure. The top and bottom layers of TPE were adhered to 254 μm fiberglass-epoxy laminate sheets with sheets of 3M® 9877 adhesive, with attached acrylic fixtures to hold these plates in the Instron® jaws. The top and bottom plates were spaced 10 mm apart before negative pressure was applied. Negative pressure was measured using a pressure sensor manifold (MPX4115V, Motorola Freescale Seminconductor, Inc., USA) and the retractive force was measured by the load cell of the Instron®. This test was performed for bellows actuators with internal PTFE disks of 254 μm thickness and otherwise identical actuators with 76.2 μm internal PTFE disks.

B. Vacuum Gripper Testing

Vacuum grippers cast from silicone elastomers in 3D-printed molds were fixtured in a fiberglass-epoxy and acrylic jig to firmly retain the gripper and affix it to the movable vertical axis of the Instron®. Vacuum was applied (92 kPa) once the base of the vacuum gripper was in contact with a sample of porcine stomach tissue. Once the gripper had retracted a portion of the porcine stomach tissue, the movable plate of the Instron® was raised vertically at a rate of 20 mm/min. Incrementally larger masses of tissue were lifted until the vacuum gripper could no longer fully raise the tissue from its enclosing container.

C. Pop-up Structure Testing

Pop-up structures and their component material selections described in Section II. and shown in Fig. 3 (d) and (e) were evaluated by comparing performance relative to desired expanded height, and desired stiffness of the overall structure.

D. Integrated Device Testing

The integrated device was deployed from an Olympus CF-100L endoscope onto porcine stomach tissue samples using an FEP (Fluorinated Ethylene Propylene) tube to serve as an overtube to contain the integrated device, as described in Fig. 1 (a) and (b). This added diameter is comparable to commercially available endoscopes in common use, which have outside diameters ranging from 12.2 - 21 mm [15]. Placing the device with thickness of 4.70 mm and width of 10 mm tangential to the outer surface of the endoscope increases the effective endoscope diameter to 20 mm, but future work on geometric design changes could decrease this diameter to operate with a smaller overtube. Negative pressure (92 kPa) was applied through the vacuum gripper to anchor the device to the tissue before the two bellows actuators were concurrently inflated.

The structure of porcine stomach is comprised of mucosa and muscularis layers which together measure 2500 μm thick. This is thicker than reported thicknesses of human GI tract mucosa and muscularis layers of the intestinal wall, which vary from 495-1090 μm, thus making porcine stomach an acceptable substitute for benchtop *ex vivo* testing [16]. Using conventional endoscopy tools, the retracted porcine stomach tissue was successfully contacted by tools inserted through the endoscope working channel.

IV. RESULTS & DISCUSSION

Prototypes of the bellows actuators with internal rigid PTFE disks are shown in Fig. 3 (a). The deflated height of the four-stage bellows without rigid internal disks is 0.85 mm with an expanded height of 18 mm; the deflated height of the comparable actuator with internal disks is 1.8 mm with a comparable expanded height.

A. Bellows Actuator Force Characterization (Extension)

In extension, four-stage bellows actuators could produce 10 N of force when expanding from fully flat. The relationship between pressure and area as $F = P \times A$ holds at low displacement heights, and can be better described as $\Delta F = \Delta P \times A$, with the rate of force increasing with a marginal increase in pressure remaining constant across various displacement heights. Regardless of total height, forces on the order of Newtons were produced. Based upon the $\Delta F = \Delta P \times A$ relationship, given the average slope of the plot in Fig. 4, the effective area is found to be 41.7 ± 8.46 mm^2. This yields an experimental result for diameter of 7.29 mm, which is 8.88% less than the diameter of the rigid PTFE disk (8 mm) and 19% less than that of the bellows chamber (9 mm).

The above slope data for calculating marginal force exerted with a change in pressure can be combined with displacement results shown in Fig. 5 to generate an expression for the observed behavior of the bellows actuator. To determine the force to be exerted at a particular height of an actuator with a 9 mm outer diameter and embedded rigid disk, the required pressure value can be interpolated from Fig. 5, or approximated by a linear fit, with the linear change added to this fixed offset. This means that

$$F = (4.17 \times 10^{-5})(\Delta P) \tag{2}$$

where $\Delta P = P_{input} - P_{Disp}$, the difference between final input pressure and the displacement pressure required for the bellows actuator to reach a particular height. The slope here results from Fig. 4 and P_{Disp} is the interpolated pressure required for the bellows actuator to reach a particular height. P_{Disp} can be found with a linear model fitted to the displacement vs. pressure data, which holds with an R-square value of 0.990 at displacements greater than 6 mm. The linear model

$$H_{Disp} = (4.78 \times 10^{-2})(P_{Disp}) + 5.41 \tag{3}$$

can be used in conjunction with Eqn. 2 to get an estimate of the forces these actuators can produce at large

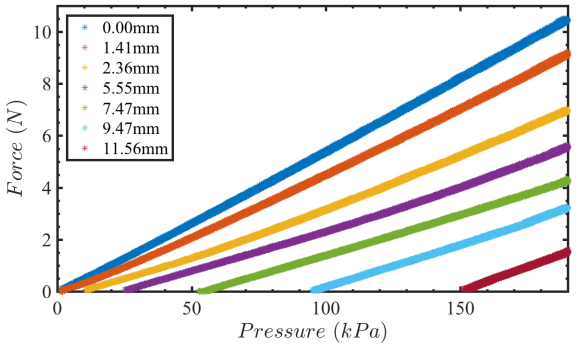

Fig. 4. Plot of pressure vs. force for four-stage bellows actuators in extension at various displacement heights.

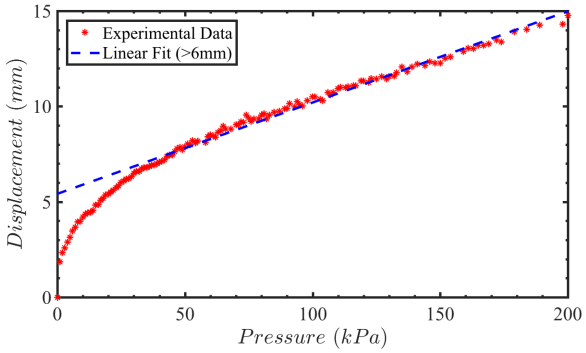

Fig. 5. Plot of displacement (mm) vs. pressure (kPa) during inflation of a four-stage bellows actuator with top and bottom TPE faces attached to 381 μm FR4 with 3M® 9877 sheet adhesive.

displacements, above 6 mm. Below this displacement, the simple $F = P \times A$ model described previously could be used to estimate the forces produced. The linear fit above 6 mm of displacement is sufficient for a device such as this, because we assume that the forces applied at large displacements (to sustain tissue retraction) are more important than those applied at small displacements. 2 mm of bellows actuator displacement is necessary for the base of the device to contact the tissue, due to the height of the vacuum gripper. This model is limited because the actuators deform when encountering resistance, but is presented as a useful way to estimate forces produced in a particular configuration.

B. Bellows Actuator Force Characterization (Retraction)

When fixtured in an extended state with top and bottom layers of the bellows constrained 10 mm apart, the maximum force outputted by a four-stage bellows actuator with rigid internal PTFE disks peaked at 3.1 N. The drop in force output after the peak value results from time-dependent behavior of the actuators as they continually buckle and compress inwards with

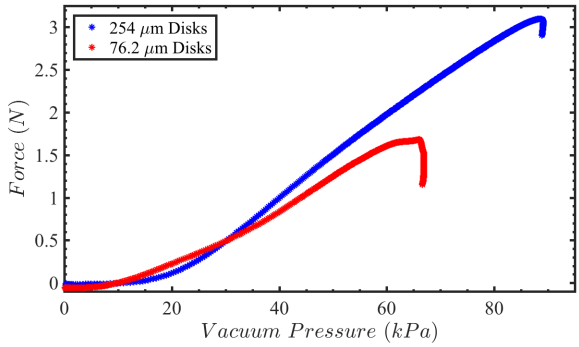

Fig. 6. Plot of pressure vs. force for four-stage bellows actuators in retraction, with rigid internal disks of different thicknesses. Top and bottom TPE faces are bonded to FR4 sheets and fixed at 10 mm displacement.

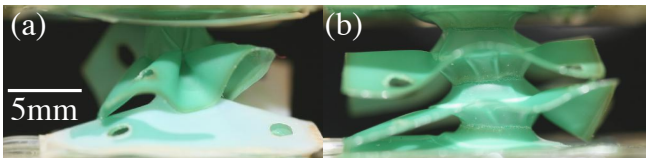

Fig. 7. (a) Bellows actuator with internal PTFE film undergoing buckling during retraction testing with applied vacuum. (b) Bellows actuator with rigid internal disks resisting buckling under applied vacuum.

sustained negative pressure. Internal disks of 254 μm thickness resulted in a peak force output of 3.10 N compared to 1.68 N for an otherwise identical actuator with 76.2 μm internal disks, as shown in Fig. 6. This represents a 1.8-fold increase in applied force by bellows actuators in retraction, a substantial increase in force exerted compared to prior versions of these actuators with thinner TPE and PTFE layers [10], validating the prediction made from Eqn. 1. The buckling of actuators with 76.2 μm internal disks is shown in Fig. 7 (a), and the resistance to buckling for actuators with 254 μm internal disks is visible in Fig. 7 (b).

C. Vacuum Gripper Lifting Characterization

Vacuum grippers made from a cast silicon elastomer were successful in lifting 40 g masses of porcine stomach tissue, corresponding to exerted forces in excess of 0.40 N. This is comparable to those measured in the literature for similar grippers that produced up to 1.2 N [17] [18].

D. Integrated Device Retracting Tissue

The integrated device was placed inside an FEP overtube (23.81 mm outer diameter and 22.23 mm inner diameter) with the Olympus CF-100L endoscope (Fig. 8 (a)). Following the scheme described in Fig. 1, the overtube was retracted from the endoscope to expose the device, as shown in Fig. 8 (b). This proof-of-concept demonstration of deployment validates the

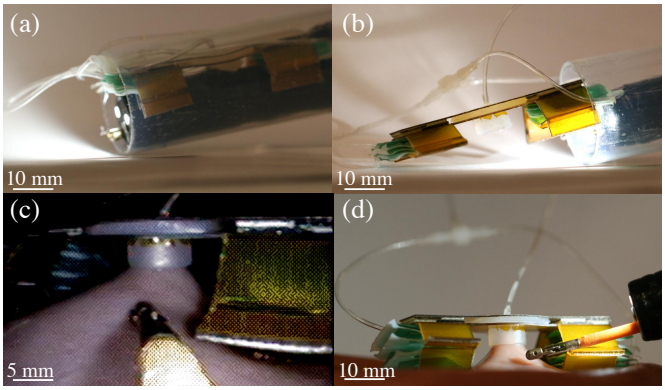

Fig. 8. (a) Integrated device encased in 23.81 mm outer diameter overtube (b) Integrated device during deployment and overtube retraction (c) View from endoscope distal camera, end-effector in foreground (d) Deployed device retracting tissue, endoscope with tool contacting tissue retracted by integrated device, as an electro-cautery tool would be used to ablate tissue.

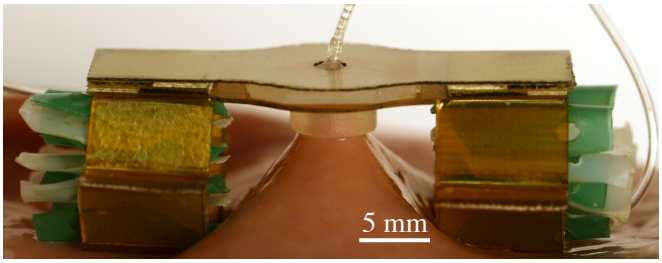

Fig. 9. Integrated device deployed on porcine stomach tissue. Tissue is retracted to height of 13.5 mm.

described workflow as a means of conducting the device to the site of a lesion. The vacuum gripper is then actuated with applied negative pressure, and inflation of the soft bellows actuators begins, retracting the porcine stomach tissue, as shown in Fig. 9. An end-effector is deployed through the working channel of the endoscope, which is capable of interacting with the retracted tissue with visual feedback provided by the endoscope distal illuminated camera, as shown in Fig. 8 (c). See attached video of synchronized distal and external camera views of the endoscope end-effector interacting with the retracted tissue.

As is visible in Fig. 8 (d), the tip of the endoscope is decoupled from the integrated tissue retraction device (linked only by flexible tubing for the vacuum gripper and soft bellows actuators). This is a major strength of the device, as once the device is deployed and retracting tissue, the surgeon is free to manipulate the endoscope to best approach the retracted tissue for electro-cautery and biopsy.

Although the integrated device successfully retracts tissue without causing damage to the surrounding area, one major limitation of pop-up book MEMS devices deployed in living systems is the sharp, planar nature of the laser micro-machined layers. Future work could be done to minimize this shortcoming by changing the geometric design of the device and adding fillets to the corners or encasing the structure in a layer of soft silicone elastomer.

V. CONCLUSIONS

In this paper, we present a device fabricated with pop-up book MEMS techniques to retract tissue in the GI tract while remaining decoupled from the endoscope tip. We introduce a layer-by-layer manufacturing method for using heat and pressure to bond TPE sheets to create pockets with sufficient depth to contain a rigid PTFE disk within each chamber of a larger bellows actuator, using PTFE forms to deform the TPE while at elevated temperatures. The manufacturing method allows for batch fabrication, as well as the inclusion of additional bellows chambers to customize the final stroke of the actuator. All proposed systems are characterized thoroughly and are fabricated with materials previously used in the fabrication of medical devices.

The inclusion of internal rigid planar disks expands the capabilities of soft TPE bellows actuators, increasing the potential use cases for a mostly-soft bidirectional actuator. On the millimeter-to-centimeter scale, soft TPE bellows offer a relatively large stroke and the ability to exert sustained forces. Furthermore, the bellows actuator design offers the potential to exert proportionally larger forces at the centimeter-scale with similarly large flat-to-expanded ratios, if designed and fabricated with larger bellows chambers.

We also introduce a retraction device which can be deployed from conventionally used endoscopes to provide the necessary counteraction to ablate tissue, paving the way for applications in endoscopic removal of early stage cancers. The integrated tissue retraction device offers surgeons an additional method to simplify endoscopic procedures, potentially solving the issues of limited distal tip dexterity and the extensive training requirements to perform these procedures. Future work could adapt the device to retract larger portions of tissues using a row or array of vacuum grippers to excise larger lesions, as well as exploring the use of the inflatable bellows actuators described here for other procedures where an initially-flat device capable of substantial expansion and exertion of force as a distance is beneficial, such as collapsed lungs or airways, as well as further applications in the GI tract. Furthermore, porcine *in vivo* testing will be performed to verify device performance in a living system and to evaluate procedure outcomes resulting from the use of the presented device.

ACKNOWLEDGMENT

The authors would like to acknowledge Harvard School of Engineering and Applied Sciences and the Wyss Institute for Biologically-Inspired Engineering for their support of this work. The authors would also like to acknowledge DARPA (grant FA8650-15-C-7548). We

would also like to thank Daniel Vogt for help with actuator batch fabrication consistency, Kaitlyn Becker for help with high-level vacuum gripper design, and Joshua Gafford for technical assistance and advice.

REFERENCES

[1] V. Vitiello, "Emerging Robotic Platforms for Minimally Invasive Surgery," *Biomedical Engineering, IEEE Reviews in*, vol. 6, pp. 111–126, 2013.

[2] A. Loeve, P. Breedveld, and J. Dankelman, "Scopes too flexible and too stiff," *IEEE Pulse*, vol. 1, no. 3, pp. 26–41, 2010.

[3] S. V. Kantsevoy, D. G. Adler, J. D. Conway, D. L. Diehl, F. A. Farraye, R. Kwon, P. Mamula, S. Rodriguez, R. J. Shah, L. M. Wong Kee Song, and W. M. Tierney, "Endoscopic mucosal resection and endoscopic submucosal dissection," *Gastrointestinal Endoscopy*, vol. 68, no. 1, pp. 11–18, 2008.

[4] J. Gafford, T. Ranzani, S. Russo, H. Aihara, C. Thompson, R. Wood, and C. Walsh, "Snap-on robotic wrist module for enhanced dexterity in endoscopic surgery," in *2016 IEEE International Conference on Robotics and Automation (ICRA)*. IEEE, 5 2016, pp. 4398–4405. [Online]. Available: http://ieeexplore.ieee.org/document/7487639/

[5] R. Nakadate, S. Nakamura, T. Moriyama, H. Kenmotsu, S. Oguri, J. Arata, M. Uemura, K. Ohuchida, T. Akahoshi, T. Ikeda, and M. Hashizume, "Gastric endoscopic submucosal dissection using novel 26-mm articulating devices: an ex vivo comparative and in vivo feasibility study," *Endoscopy*, vol. 47, no. 9, pp. 820–824, 2015.

[6] G. P. Mylonas, V. Vitiello, T. P. Cundy, A. Darzi, and G. Z. Yang, "CYCLOPS: A versatile robotic tool for bimanual single-access and natural-orifice endoscopic surgery," *Proceedings - IEEE International Conference on Robotics and Automation*, pp. 2436–2442, 2014.

[7] S. Konishi, S. Sawano, N. Fujiwara, Y. Kurumi, and T. Tani, "Outer shell actuator driving central bending shaft by balloon arrays circumferentially-arranged inside of shell," *TRANSDUCERS 2009 - 15th International Conference on Solid-State Sensors, Actuators and Microsystems*, pp. 53–56, 2009.

[8] S. Russo, T. Ranzani, J. Gafford, C. J. Walsh, and R. J. Wood, "Soft pop-up mechanisms for micro surgical tools: Design and characterization of compliant millimeter-scale articulated structures," in *Proceedings - IEEE International Conference on Robotics and Automation*, vol. 2016-June, 2016, pp. 750–757.

[9] D. Hellier, F. Albermani, B. Evans, H. de Visser, C. Adam, and J. Passenger, "Flexural and torsional rigidity of colonoscopes at room and body temperatures," *Proceedings of the Institution of Mechanical Engineers, Part H: Journal of Engineering in Medicine*, vol. 1, no. -1, pp. 1–11, 2011.

[10] T. Ranzani, S. Russo, F. Schwab, C. J. Walsh, and R. J. Wood, "Deployable Stabilization Mechanisms for Endoscopic Procedures," in *Proceedings of Robotics and Automation (ICRA), 2017 IEEE International Conference on.*, 2017.

[11] J. P. Whitney, P. S. Sreetharan, K. Y. Ma, and R. J. Wood, "Pop-up book MEMS," *Journal of Micromechanics and Microengineering*, vol. 21, no. 11, p. 115021, 2011.

[12] J. Gafford, T. Ranzani, S. Russo, A. Degirmenci, S. Kesner, R. D. Howe, R. J. Wood, and C. Walsh, "Towards Medical Devices with Integrated Mechanisms, Sensors and Actuators via Printed-Circuit MEMS," *Journal of Medical Devices*, no. January, 2016. [Online]. Available: http://medicaldevices.asmedigitalcollection.asme.org/article.aspx?doi=10.1115/1.4035375

[13] L. Paez, G. Agarwal, and J. Paik, "Design and Analysis of a Soft Pneumatic Actuator with Origami Shell Reinforcement," *Soft Robotics*, vol. 3, no. 3, pp. 109–119, 2016. [Online]. Available: http://online.liebertpub.com/doi/10.1089/soro.2016.0023

[14] R. J. Roark, W. C. Young, and R. Plunkett, *Formulas for Stress and Strain*, 1976, vol. 7. [Online]. Available: http://appliedmechanics.asmedigitalcollection.asme.org/article.aspx?articleid=1403104

[15] W. M. Tierney, D. G. Adler, J. D. Conway, D. L. Diehl, F. A. Farraye, S. V. Kantsevoy, V. Kaul, S. R. Kethu, R. S. Kwon, P. Mamula, M. C. Pedrosa, and S. A. Rodriguez, "Overtube use in gastrointestinal endoscopy," *Gastrointestinal Endoscopy*, vol. 70, no. 5, pp. 828–834, 2009.

[16] C. H. Huh, M. S. Bhutani, E. B. Farfán, and W. E. Bolch, "Individual variations in mucosa and total wall thickness in the stomach and rectum assessed via endoscopic ultrasound." *Physiological measurement*, vol. 24, no. 4, pp. N15–N22, 2003.

[17] Toshiaki Horie, Satoshi Sawano, and Satoshi Konishi, "Micro switchable sucker for fixable and mobile mechanism of medical MEMS," in *2007 IEEE 20th International Conference on Micro Electro Mechanical Systems (MEMS)*, no. January. IEEE, 1 2007, pp. 691–694. [Online]. Available: http://ieeexplore.ieee.org/document/4433169/

[18] T. Ranzani, S. Russo, C. Walsh, and R. Wood, "A soft suction-based end effector for endoluminal tissue manipulation," in *The Hamlyn Symposium on Medical Robotics*, 2016, pp. 3–4.